Article

SOURCE DATA | TRANSPARENT PROCESS

THE EMBO JOURNAL

Modulation of Yorkie activity by alternative splicing is required for developmental stability

Diwas Srivastava, Marion de Toledo, Laurent Manchon, Jamal Tazi & François Juge*

Abstract

The Hippo signaling pathway is a major regulator of organ growth, which controls the activity of the transcription coactivator Yorkie (Yki) in *Drosophila* and its homolog YAP in mammals. Both Yki and YAP proteins exist as alternatively spliced isoforms containing either one or two WW domains. The biological importance of this conserved alternative splicing event is unknown. Here, we identify the splicing factor B52 as a regulator of *yki* alternative splicing in *Drosophila* and show that B52 modulates growth in part through modulation of *yki* alternative splicing. Yki isoforms differ by their transcriptional activity as well as their ability to bind and bridge PPxY motifs-containing partners, and can compete *in vivo*. Strikingly, flies in which *yki* alternative splicing has been abrogated, thus expressing only Yki2 isoform, exhibit fluctuating wing asymmetry, a signal of developmental instability. Our results identify *yki* alternative splicing as a new level of modulation of the Hippo pathway, that is required for growth equilibration during development. This study provides the first demonstration that the process of alternative splicing contributes to developmental robustness.

Keywords alternative splicing; developmental stability; growth; hippo pathway

Subject Categories Chromatin, Transcription & Genomics; Development; RNA Biology

DOI 10.15252/embj.2020104895 | Received 4 March 2020 | Revised 21 October 2020 | Accepted 6 November 2020 | Published online 15 December 2020

The EMBO Journal (2021) 40: e104895

Introduction

The Hippo signaling pathway is a conserved pathway that regulates cell fate and cell proliferation to control organ growth and regeneration (Misra & Irvine, 2018; Zheng & Pan, 2019). The core of the pathway comprises a kinase cascade including Hippo (Hpo, MST1/2 in mammals; Harvey *et al*, 2003; Jia *et al*, 2003; Pantalacci *et al*, 2003; Wu *et al*, 2003; Udan *et al*, 2003) and Warts (Wts, LATS1/2 in mammals; Justice *et al*, 1995; Xu *et al*, 1995), which phosphorylate the transcriptional coactivator Yorkie (Yki, YAP in mammals; Huang *et al*, 2005). Yki/YAP is a shuttling protein (Elosegui-Artola *et al*, 2017; Manning *et al*, 2018), and the phosphorylation status of Yki/YAP has a major impact on its nucleo/cytoplasmic distribution. Phosphorylation of Yki/YAP at S168/S127 allows binding to 14.3.3 proteins and accumulation into the cytoplasm (Dong *et al*, 2007; Zhao *et al*, 2007; Oh & Irvine, 2008). Upon inactivation of the pathway, unphosphorylated Yki/YAP accumulates into the nucleus where it activates a transcriptional program promoting cell proliferation and inhibiting apoptosis. Yki/YAP does not bind DNA directly but interacts with specific transcription factors, especially members of the TEAD family Scalloped (Sd) in flies and TEAD1/2/3/4 in mammals (Wu *et al*, 2008; Zhang *et al*, 2008; Goulev *et al*, 2008; Zhao *et al*, 2008). Nuclear Yki/YAP then recruits multiple transcriptional regulators including the histone methyl-transferase NcoA6 to trigger transcription activation (Qing *et al*, 2014; Oh *et al*, 2014). In addition, Yki was proposed to displace the transcriptional repressor Tgi (Tondu-domain-containing Growth Inhibitor, SDBP in mammals) from Sd/TEAD and relieve a transcriptional repression (Guo *et al*, 2013; Koontz *et al*, 2013). Yki/YAP interacts with its partners through different domains: the N-terminal domain binds Sd/TEAD whereas the two WW domains mediate interaction with PPxY motifs-containing proteins such as the repressor Tgi and the transactivator NcoA6 for example. Interestingly, both Yki and YAP exist as two isoforms containing either one or two WW domains, owing to the alternative splicing of an exon encoding the second WW domain (Komuro *et al*, 2003; Huang *et al*, 2005). In mammals, YAP isoform with only one WW domain cannot bind angiomotin or p73 indicating that alternative splicing could play a role in the modulation of YAP activity (Oka *et al*, 2008, 2012). Up to now, the molecular bases and as well as the functional importance of this alternative splicing event *in vivo* are unknown.

Here, we identify *yki* as an alternative splicing target of the splicing factor B52 in *Drosophila* and functionally address the importance of *yki* alternative splicing *in vivo*. The B52 protein belongs to the family of Serine and arginine-rich (SR) proteins that are conserved RNA-binding proteins involved in several steps of mRNA metabolisms and which play a major role in both constitutive and alternative splicing (Howard & Sanford, 2015). We previously showed that, in *Drosophila*, the level of B52 protein influences cell growth (Fernando *et al*, 2015), but the underlying molecular mechanisms were not characterized. Here, we show that B52 is necessary for the inclusion of *yki* alternative exon and that B52's depletion reduces growth in part through modulation of *yki* alternative splicing. We further show that alternative inclusion of Yki second WW domain is an

Institut de Génétique Moléculaire de Montpellier, University of Montpellier, CNRS, Montpellier, France
*Corresponding author. Tel: +33 04 34 35 99 77; E-mail: francois.juge@inserm.fr

additional level of modulation of Yki activity that is unexpectedly required for correct growth equilibrium between the right and left sides of *Drosophila*. These results identify the first alternative splicing event involved in developmental robustness.

Results

yki alternative splicing is a target of B52

We previously observed that B52 depletion reduces cell growth in *Drosophila* larvae salivary glands as well as in the thorax at later stages (Fernando *et al*, 2015). We reasoned that B52's effect on growth might be due to alternative splicing modulation of one or several genes controlling growth. To identify splicing events that are robustly affected by B52 depletion, we cross-compared two previously published RNA-seq datasets corresponding to RNAi-mediated depletion of B52 in S2 cells and to control cells (Bradley *et al*, 2015; Brooks *et al*, 2015). We used MAJIQ (Modeling Alternative Junction Inclusion Quantification; Vaquero-Garcia *et al*, 2016) to identify Local Splicing Variations (LSV) that vary more than 20% between control and B52 RNAi conditions, in both datasets (see Methods). This identified 108 high-confidence splicing events in 105 genes (Fig 1A and Appendix Table S1). Remarkably, 24 genes encode proteins that have direct or indirect interaction(s) with another protein in the list, thus identifying 11 groups containing two to three interacting proteins (Fig 1B). This high number of groups is highly significant ($P < 2e\text{-}5$) and shows that B52 tends to co-regulate alternative splicing of genes encoding protein partners. GO term enrichment analysis of the 105 genes identifies "regulation of organ growth" and "positive regulation of growth" as the most enriched GO terms (Fig 1C). Among them, three genes linked to the Hippo pathway were identified: *yorkie* (*yki*), *WW domain-binding protein 2* (*Wbp2*) and *Zyxin* (*Zyx*). RNA-seq data indicate that B52 depletion promotes skipping of exon 3 in *yki* mRNA, the inclusion of exons 6 and 7 in *wbp2,* and the retention of the last intron in *Zyx* (Fig EV1A–D). The functional consequences of these alternative splicing events are unknown. We focused our study on *yki* which encodes the effector of the Hippo pathway.

The exon 3 of *yki* gene encodes one of the two WW domains of the protein. Alternative inclusion of this exon leads to the production of two isoforms that we named Yki2 and Yki1 according to their number of WW domains (Fig 1D). We confirmed by RT–PCR and Western blotting that RNAi-induced depletion of B52 in S2R+ cells, or in larval wing discs, induces skipping of *yki* exon 3 and increases expression of Yki1 at the expense of Yki2 isoform (Fig 1E and 1F). Ubiquitous depletion of B52 in larvae reduces Yki2/Yki1 ratio from 7.1 ± 0.6 to 3.3 ± 0.6 without significantly affecting total Yki protein level (Fig EV1E). These results identify B52 as necessary for inclusion of *yki* exon 3 and expression of Yki2 isoform.

B52 depletion reduces growth and Yki activity

To test whether B52 depletion affects Yki activity, we monitored the expression of two reporter genes, *ex-lacZ* and *diap-lacZ*, which are direct targets of Yki. Expression of B52 RNAi in the posterior domain of the wing disc decreases the expression of the two reporter genes in this domain, reflecting a reduction of Yki activity (Fig 2A). This goes along with a reduction of posterior domain size. These flies are not viable at 25°C but are partially viable at 18°C and show a net reduction of wing posterior domain size (Fig 2C). Using this phenotype, we tested whether *B52* interacts genetically with the Hippo pathway. We developed V5-tagged *UAS-Yki1* and *UAS-Yki2* transgenic flies for Gal4-mediated overexpression, by site-specific integration, and confirmed that transgenic Yki1 and Yki2 isoforms are expressed at similar levels upon activation (Fig 2B). Overexpression of Yki1 or Yki2 with *hh-Gal4* driver leads to overgrowth of the posterior domain, with Yki2 giving a stronger phenotype (Fig 2C and D). Expression of Yki1 or Yki2 in *hh-Gal4>RNAi-B52* flies partially rescues the growth defect induced by B52 depletion, Yki2 being more efficient (Fig 2C and D). Similarly, depletion of the kinases Hpo or Wts by RNAi, partially rescues this phenotype (Fig 2C and D). Therefore, increasing Yki activity partially compensates the effect of B52 depletion. Nevertheless, posterior domain size in these contexts remains smaller than the corresponding controls (overexpression of Yki isoforms or depletion of Wts or Hpo in the absence of B52 depletion, Fig 2D). This suggests that B52 depletion affects other genes or pathways necessary for efficient growth. Moreover, the strong overgrowth induced by Yki overexpression, or by Hpo or Wts depletion, may compensate for a growth defect in B52-depleted cells, unrelated to the Hippo pathway. This is unlikely because depletion of Tgi, a transcriptional repressor interacting with Sd, which induces a very mild increase of posterior domain size on its own, also rescues the growth defect due to B52 depletion (Fig 2C and D). Moreover, introduction of a *UAS-GFP* transgene did not rescue the growth defect in B52-depleted wings arguing against a titration of Gal4 by extra copies of *UAS* sequences carried by the transgenes (Fig 2D). Altogether these results indicate that B52 depletion reduces growth at least in part through the Hippo pathway and suggest that it lowers Yki activity by modifying alternative splicing of *yki* mRNAs. We therefore explored the functional differences between the two Yki isoforms.

Yki1 is a weaker transcriptional activator than Yki2

Compared with Yki2 isoform, overexpression of Yki1 isoform induces weaker overgrowth phenotypes in the posterior domain of wings (Fig 2C and D) or in the eyes (Fig EV2A) suggesting that Yki1 has a weaker activity. Thus, we directly compared the ability of Yki isoforms to activate transcription in luciferase assays in S2R+ cells. Fusion of Yki to Gal4 DNA binding domain (G4DBD) induces expression of a *UAS-Luciferase* reporter (Huang *et al*, 2005). In this assay, Yki1 isoform has a 10 times weaker activity than Yki2 (Fig 3A). We next compared Yki isoforms activity on a *3xSd-Luciferase* reporter, on which Yki is recruited through the transcription factor Sd (Zhang *et al*, 2008). Both Yki1 and Yki2 activate this reporter in the presence of Sd, Yki1 having a weaker effect (about 2 fold; Fig 3A). These results show that Yki1 isoforms is a weaker transcription activator compared with Yki2 isoform.

To further compare the activity of Yki isoforms *in vivo*, we analyzed the expression of Yki reporter genes *ex-lacZ* and *diap-lacZ* following Yki isoforms overexpression in the posterior domain of wing discs. Expression of both transgenes is moderately increased by Yki1 overexpression as compared to Yki2 overexpression (Fig 3B and C). We also analyzed the expression of a *bantam* miRNA

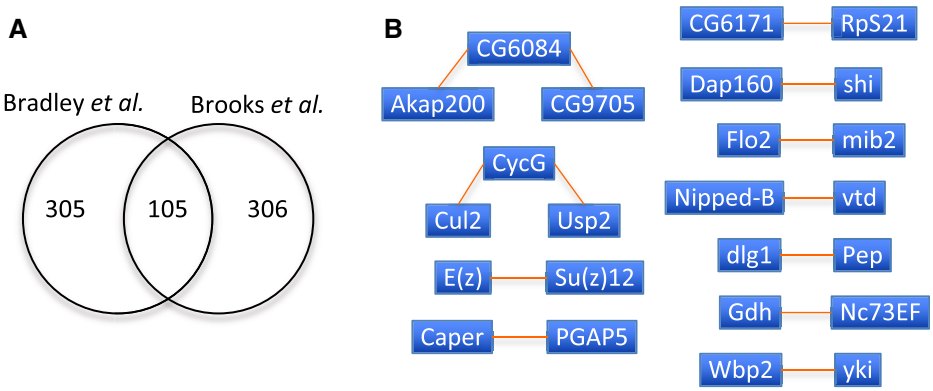

C

GO biological process	Nb of genes	Hits	Expected	Fold Enrichment	P value
regulation of organ growth	63	6	0.48	12.61	4.27E-02
positive regulation of growth	118	8	0.89	8.97	1.57E-02
regulation of catabolic process	206	11	1.56	7.07	2.26E-03
regulation of multi-organism process	173	9	1.31	6.89	3.03E-02
positive regulation of developmental process	253	13	1.91	6.80	3.11E-04
regulation of cellular catabolic process	182	9	1.37	6.55	4.46E-02
regulation of cell population proliferation	237	11	1.79	6.14	8.38E-03
positive regulation of multicellular organismal process	261	12	1.97	6.09	3.12E-03
immune system process	316	13	2.39	5.45	3.54E-03
regulation of growth	309	12	2.33	5.14	1.68E-02

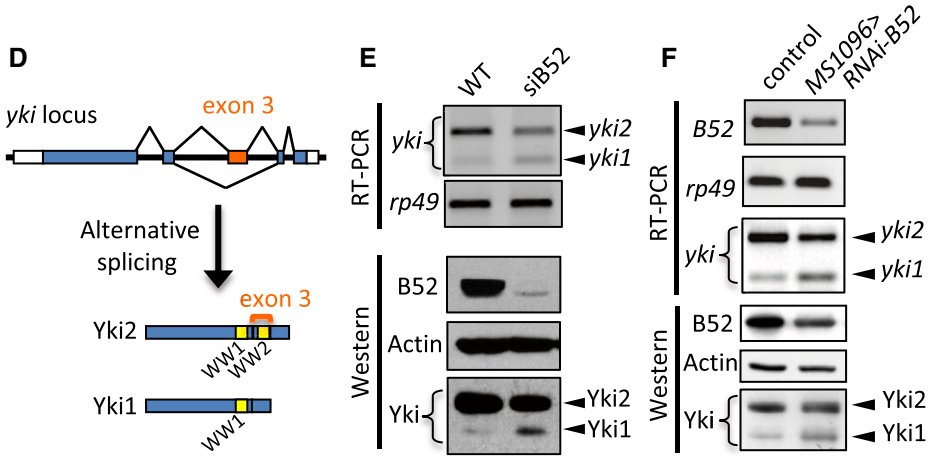

Figure 1. Identification of *yki* as a B52-regulated alternative splicing target.

A Number of genes identified by MAJIQ that display 20% or more variation in splicing between wild-type and B52 depleted cells, in each dataset. We identified 108 shared alternative splicing events, corresponding to 105 genes. A comprehensive list of the 108 events is given in Appendix Table S1.

B High-confidence protein–protein complexes identified by MIST (Molecular Interaction Search Tool) within the 105 genes identified in (A). Interactions between proteins can be direct or indirect within the complexes.

C GO term enrichment analysis of the 105 genes identified in (A), performed by PANTHER with Bonferroni correction for multiple testing.

D Schematic representation of *yki* locus and its two isoforms: Yki2 (includes exon 3 and contains 2 WW domains) and Yki1 (skips exon 3 and contains 1 WW domain).

E, F RT–PCR and Western blot showing the effect of RNAi-mediated B52 depletion in S2R+ cells (E) and in larval wing discs (F).

Source data are available online for this figure.

sensor, the expression of which is inversely correlated to the level of *ban* miRNA that is a direct target of Yki. Yki1 induces a weaker decrease of *ban*-sensor expression than Yki2 isoform (Fig 3C). Together these results show that Yki1 has a reduced activity compared with Yki2 *in vivo*.

Absence of the second WW domain modifies the binding and bridging activities of Yki

Yki1 and Yki2 isoforms differ, respectively, by the absence or presence of the alternative exon 3, which includes the second WW

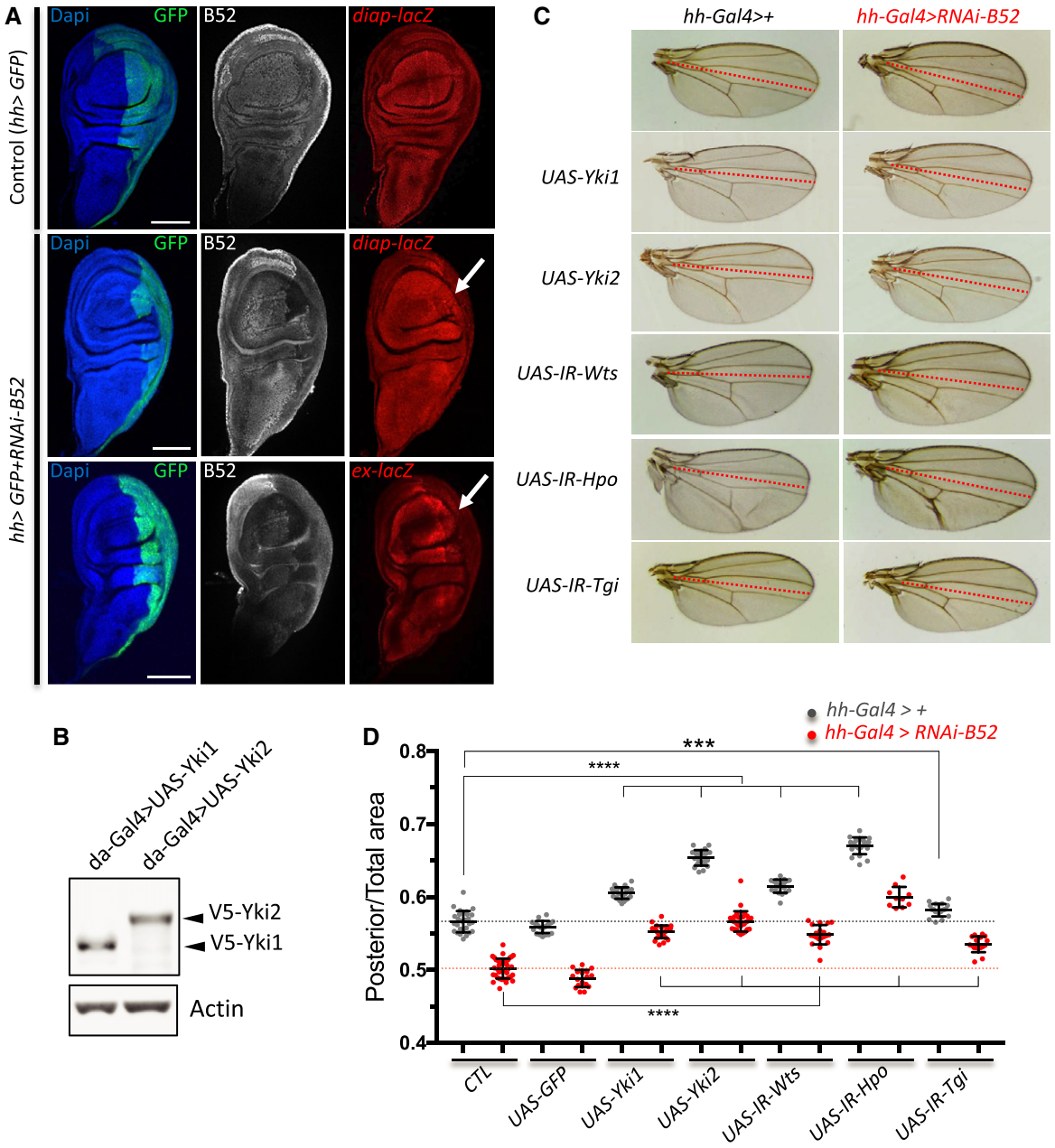

Figure 2. B52 depletion lowers Yki activity and reduces growth.

A Expression of *diap-lacZ* and *ex-lacZ* reporters upon depletion of B52 in the posterior part of the wing disc (*hh-Gal4* driver). GFP expression labels the posterior domain. Arrows highlight the reduced expression of the reporters in the posterior domain. Scale bars: 100 μm.

B Western blot showing overexpression level of V5-tagged Yki1 and V5-tagged Yki2 in total larvae, under the control of *da-Gal4* driver, probed with V5 antibody.

C Wing phenotype induced by depletion of B52 in the posterior domain of the wing disc combined with modulation of Hpo pathway. Dotted lines separate anterior (top) and posterior parts (bottom) of the wing. Flies were grown at 18°C.

D Quantification of Posterior/Total wing area in male flies of the genotypes illustrated in panel (C). *UAS-GFP* was used as a control. Each point represents a single wing, and bars represent mean with standard deviation. ***P-value < 0.001, ****P-value < 0.0001 (unpaired two-tailed t-tests). Flies were grown at 18°C.

Source data are available online for this figure.

domain. Numerous studies have demonstrated that, in the context of Yki2 isoform, WW domains are required for interaction with several partners containing PPxY motifs such as Ex, Hpo, Wts, NcoA6, Wbp2, and Tgi (Huang *et al*, 2005; Badouel *et al*, 2009; Oh *et al*, 2009; Zhang *et al*, 2011; Guo *et al*, 2013; Koontz *et al*, 2013; Oh *et al*, 2014; Qing *et al*, 2014). The absence of one WW domain in Yki1 could reduce interaction with such partners. Moreover, binding of proteins that interact with the N-terminal part of Yki, such as Sd or 14.3.3, may also be affected if the structure of the protein is modified by the absence of the domains encoded by exon 3. It is therefore

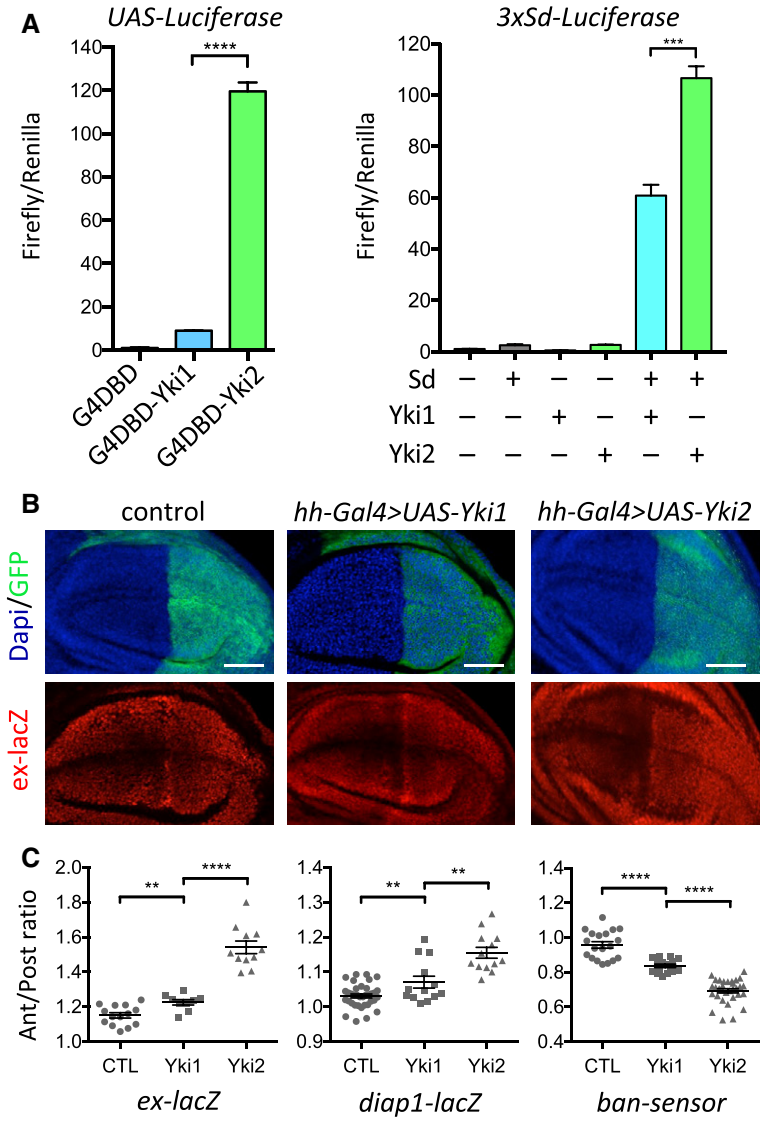

Figure 3. Yki1 isoform is a weaker transcriptional activator than Yki2 isoform.

A Comparison of Yki isoforms activity in luciferase assays using *UAS-luciferase* or *3xSd-Luciferase* reporters in S2R+ cells. Error bars represent SD, $n = 3$. ***P-value < 0.001; ****P-value < 0.0001 (unpaired two-tailed t-tests).

B Example of immunostaining used to quantify expression of *ex-lacZ* in wild type or upon Yki1 or Yki2 overexpression in wing disc posterior domain. GFP labels the posterior domain. Scale bars: 50 μm.

C Quantification of Yki reporter genes expression upon overexpression of Yki isoforms in the wing posterior domain (*hh-Gal4* driver). For each target gene, relative expression between posterior and anterior domain in the wing discs was quantified by immunostaining using anti-ßgal antibody (for *ex-lacZ* and *diap1-lacZ*) or direct visualization of GFP (*ban-sensor*, in this case posterior domain was visualized by immunostaining against V5-tag present in *UAS-Yki* transgenes). In the scatter dot plot, each symbol (circle, square and triangle) represents a single wing disc; bars represent mean with SEM. **P-value < 0.01; ****P-value < 0.0001 (unpaired two-tailed t-tests).

important to address these interactions in the context of full-length proteins and with a quantitative assay. To this end, we developed a dual-luciferase co-Immunoprecipitation (co-IP) method in S2R+ cells inspired by the DULIP method (Trepte *et al*, 2015) described in mammalian cells. Our assay monitors co-IP between a bait protein fused to Flag-tagged-Firefly Luciferase (FFL) and a prey protein fused to Renilla Luciferase (RL). Quantification of luciferase activity ratio after IP with anti-Flag antibodies gives a rapid and sensitive readout of the interaction between the bait and the prey (Fig 4A). FFL-Yki1 and FFL-Yki2 were used as baits for interactions with thirteen known Yki partners fused to RL as preys (Fig 4B). We used FFL as a control for non-specific interactions and quantified a normalized co-IP interaction (NcoIP, see methods). By this approach, we detected significant interactions between Yki isoforms and all proteins tested, from modest co-IP with GAF, MAD, and Cbt, to high and very high interactions for the other proteins. We found that both isoforms Yki1 and Yki2 interact similarly with the transcription factors Sd, MAD, Cbt, and Hth, the chromatin-associated

factors GAF and Mor, and with 14.3.3 protein (Fig 4C). These results show that interactions with these partners are not influenced by the domains encoded by *yki* exon 3. On the other hand, Yki1's interaction with Hpo, Wts, Ex, NcoA6, Wbp2, and Tgi, which all contain PPxY motif(s), is reduced compared with Yki2 (Fig 4C). Interestingly, the strength of this decrease correlates with the number of PPxY motifs present in these proteins (Fig 4C). This is in agreement with *in vitro* studies reporting cooperative binding between multiple PPxY motifs and tandem WW domains of YAP and Yki (Webb *et al*, 2011; Nyarko, 2018). Altogether these results indicate that Yki isoforms interact similarly with transcription factors but that Yki1 cannot efficiently recruit co-activators like NcoA6 or Wbp2 to stimulate transcription.

In addition to increasing the binding of proteins with multiple PPxY motifs, the presence of two WW domains may also allow Yki2 to interact simultaneously with two PPxY-containing proteins. To test this hypothesis, we compared the ability of Yki isoforms to bridge different proteins, by monitoring their co-IP using our assay. Previous reports showed that Yki binds to Sd through its N-terminal part and to Tgi *via* the WW domains (Goulev *et al*, 2008; Zhang *et al*, 2008). Moreover, Sd and Tgi were shown to interact directly (Guo *et al*, 2013; Koontz *et al*, 2013). Yki was shown to compete with Tgi for Sd binding (Guo *et al*, 2013; Koontz *et al*, 2013), but was also found in a trimeric complex with Sd and Tgi (Guo *et al*, 2013). We, therefore, monitored Sd/Tgi interaction in the absence or presence of Yki isoforms in transfected cells (Fig 4D). Using FFL-Sd as bait, we detected co-IP between FFL-Sd and Tgi-RL in the absence of Yki. Both Yki1 and Yki2 isoforms enhanced the co-IP between Sd and Tgi, with Yki2 having a stronger effect. The stronger effect of Yki2 could reflect an increased stability of the complex or the recruitment of an additional Tgi molecule through the second WW domain. Point mutations in the two WW domains of Yki2 abolish its effect on Sd-Tgi co-IP (Fig 4D). These results are in agreement with the existence of a trimeric complex between Sd, Tgi, and one isoform of Yki.

To further test Yki's bridging activity, we analyzed the co-IP between FFL-Sd and RL-Wbp2 by the same approach. The co-transfection of Yki1 or Yki2 increases the pull-down between Sd and Wbp2, with Yki2 having a stronger effect. Mutation of both WW domains in Yki2 abrogates this effect (Fig 4E). These results indicate that, in interaction with Sd, both Yki1 and Yki2 isoforms participate in the recruitment of Tgi or Wbp2, with Yki2 being more efficient owing to its two WW domains. Finally, we tested if the two WW domains of Yki2 can interact with two different proteins carrying PPxY motifs. To this end, we analyzed the co-IP between Tgi and Wbp2 using FFL-Tgi as bait and RL-Wbp2 as prey. Remarkably, Yki2 isoform allowed to pull-down Wbp2 with Tgi, whereas Yki1 isoform did not. As expected, mutation of the two WW domains in Yki2 abrogates the co-IP (Fig 4F). Altogether these results show that the presence of the second WW domain in Yki2 isoform increases the interactions with PPxY motifs-containing proteins and allows Yki2 to bridge two different proteins with such motifs.

Yki isoforms can compete with each other in the nucleus

Our results show that, compared with Yki2 isoform, Yki1 isoform interacts similarly with the transcription factors, but less with the transcription co-activators NcoA6 and Wbp2, providing an explanation to its lower transcriptional activity. This suggests that Yki isoforms may compete with each other for binding to the transcription factors. To test this hypothesis, we analyzed the expression of the *3xSd-Luciferase* reporter in the presence of Yki1, Yki2, or combinations of both isoforms (Fig 4G). Co-transfection of increasing amount Yki2 in the presence of Yki1 increases expression of the reporter. On the contrary, co-transfection of increasing amount of Yki1 in the presence of Yki2 decreases reporter expression. These results strongly suggest that Yki isoforms can compete for binding to Sd and for activating transcription.

To directly test whether Yki1 isoform can compete with Yki2 isoform *in vivo*, we co-overexpressed them in the eye. We used wild-type forms of Yki isoforms as well as activated versions of these isoforms, carrying the mutation S168A that kills a Wts phosphorylation site (Dong *et al*, 2007). We verified that this mutation favors the nuclear accumulation of both $Yki1^{S168A}$ and $Yki2^{S168A}$ isoforms (Fig EV3A and B) and increases the overgrowth phenotypes induced by overexpression of these isoforms in the eye (Fig EV2A). Of note, activated $Yki1^{S168A}$ induces dramatically weaker overgrowth compared with $Yki2^{S168A}$ confirming its reduced transcriptional activity. Overexpression of $Yki2^{S168A}$ in the eye induces strong overgrowth and remarkably, co-overexpression of activated $Yki1^{S168A}$, but not non-activated form Yki1, reduces this phenotype (Figs 4H and EV2B), providing evidence of competition between the two isoforms in the nucleus. Altogether our results are in agreement with a competition model between a fully active isoform Yki2 and a less-active isoform Yki1.

B52's effect on growth involves *yki* alternative splicing

Our results show that B52 depletion reduces growth (Fig 2) and promotes expression of Yki1 isoform through modulation of *yki* alternative splicing (Fig 1). To directly determine whether this contributes to the effect of B52 on growth, we abrogated alternative splicing of *yki* exon 3 by creating flies producing exclusively Yki2 isoform. To this end, we edited endogenous *yki* locus to replace the central part of the gene by a portion of *yki2* cDNA, therefore eliminating the introns surrounding exon 3 (Fig 5A, see strategy in Fig EV4). We generated two $yki^{2\text{-}only}$ alleles, $yki^{2\text{-}only\text{-}A}$ and $yki^{2\text{-}only\text{-}B}$, corresponding to two independent gene conversion events, which show identical phenotypes. Homozygous $yki^{2\text{-}only}$ flies are viable, and we confirmed by Western blotting that $yki^{2\text{-}only}$ flies express only Yki2 isoform and do not produce Yki1 isoform (Fig 5B). Remarkably, depletion of B52 in wing posterior domain in $yki^{2\text{-}only}$ background induces a weaker phenotype than in a wild-type background (Fig 5C). Nevertheless, overall wing size remains significantly smaller than wild type. This result indicates that B52's effect on growth is in part due to the modulation of *yki* alternative splicing as well as to other targets.

Despite being viable to adulthood, we observed that $yki^{2\text{-}only}$ embryos display about 50% lethality (Fig 5D). This lethality is due to a maternal effect since it appears when $yki^{2\text{-}only}$ females are crossed with wild-type males, but not in the reverse cross (Fig 5D). This suggests an important role of Yki1 isoform and/or *yki* alternative splicing in oogenesis or early embryonic development. This phenotype was not investigated further, since we focused on an asymmetry phenotype observed in adults, as described below.

Since Yki1 is less active than Yki2 isoform (Fig 3) and can compete with it (Fig 4), we asked whether the absence of Yki1

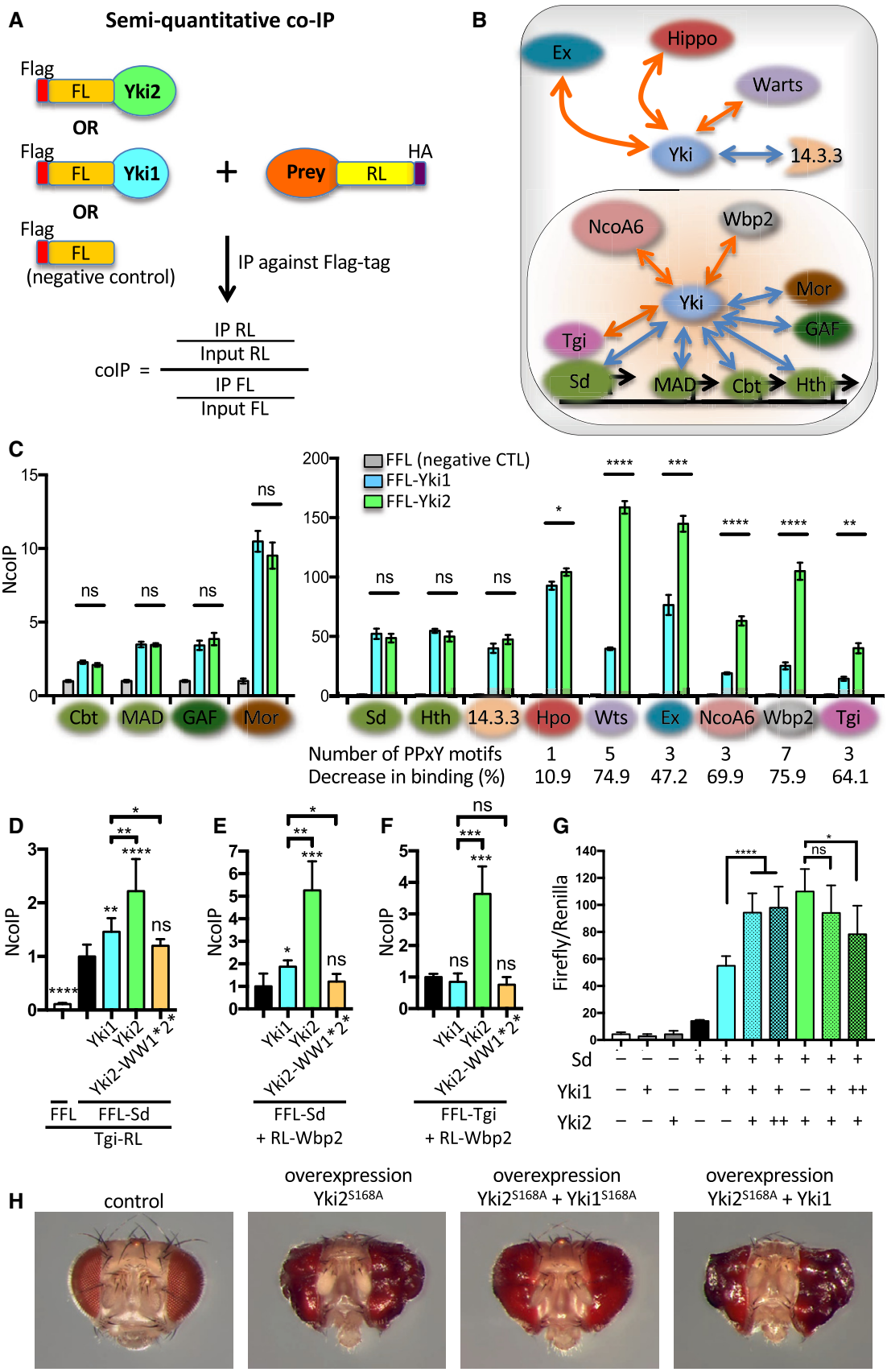
A
Semi-quantitative co-IP
Flag
FL
Yki2
OR
Flag
FL
Yki1
OR
Flag
FL
(negative control)
+
Prey
RL
HA
IP against Flag-tag
coIP = IP RL / Input RL / IP FL / Input FL
B
Ex
Hippo
Warts
Yki
14.3.3
NcoA6
Wbp2
Mor
Yki
GAF
Tgi
Sd
MAD
Cbt
Hth
C
NcoIP
FFL (negative CTL)
FFL-Yki1
FFL-Yki2
ns
Cbt
MAD
GAF
Mor
Sd
Hth
14.3.3
Hpo
Wts
Ex
NcoA6
Wbp2
Tgi
Number of PPxY motifs 1 5 3 3 7 3
Decrease in binding (%) 10.9 74.9 47.2 69.9 75.9 64.1
D
E
F
NcoIP
Yki1
Yki2
Yki2-WW1*2*
FFL
FFL-Sd
Tgi-RL
FFL-Sd
+ RL-Wbp2
FFL-Tgi
+ RL-Wbp2
G
Firefly/Renilla
Sd
Yki1
Yki2
H
control
overexpression
Yki2S168A
overexpression
Yki2S168A + Yki1S168A
overexpression
Yki2S168A + Yki1

Figure 4.

Figure 4. Yki1 isoform lacks some bridging activity and can compete with Yki2 isoform in the nucleus.

A Principle of dual-luciferase co-IP. In all experiments, IP is performed against the Flag-tag fused to the Firefly Luciferase (FFL). FFL (unfused to Yki) is used as reference to normalize each interaction. The prey protein is fused to Renilla Luciferase (RL) in C-term for most proteins or in N-term (for Wbp2 and Mor).

B Drawing of the monitored protein–protein interactions. Interactions previously shown to involve WW domains are indicated by orange arrows, whereas other interactions are schematized by blue arrows.

C Comparison of Yki isoforms binding capabilities by dual-luciferase co-IP. Graphs show the normalized co-IP (NcoIP) results for 13 proteins tested against the two Yki isoforms and the negative control (Flag-Firefly).

D Interaction between Sd and Tgi in the absence or presence of Yki isoforms.

E Interaction between Sd and Wbp2 in the absence or presence of Yki isoforms.

F Interaction between Tgi and Wbp2 in the absence or presence of Yki isoforms.

G Luciferase assay using *3xSd-Luciferase* reporter in S2 cells, transfected with single or combination of Yki isoforms. Error bars represent SD, $n = 6$. *P-value < 0.05; ****P-value < 0.0001 (unpaired two-tailed t-tests).

H Co-overexpression of Yki isoforms using *GMR-Gal4* driver provides evidence of competition between Yki isoforms.

Data information: In (C, D, E, and F), bars represent mean and error bars represent SD, $n = 4$. P-values: *$P < 0.05$, **$P < 0.01$, ***$P < 0.001$, ****$P < 0.0001$ (unpaired two-tailed t-tests).

would lead to growth advantage. We did not detect overgrowth in $yki^{2\text{-}only}$ adult flies. Therefore, we addressed whether the absence of Yki1 isoform influences growth in clonal assays in the wing disc. In this assay, wild-type sibling cells generated by mitotic recombination give rise to clones of similar size (Fig 5E). On the other hand, homozygous $yki^{2\text{-}only\text{-}A}$ cells, obtained by mitotic recombination in heterozygous $yki^{2\text{-}only\text{-}A}/yki^{+}$ larvae, often create bigger clones than their sibling wild-type yki^{+}/yki^{+} cells (Fig 5F). In few cases, yki^{+}/yki^{+} sibling clones were not recovered, suggesting that these cells were eliminated. These results indicate that the absence of Yki1 in $yki^{2\text{-}only}$ cells increases overall Yki activity and are in agreement with a model of Yki1 isoform acting as a dimmer of Yki activity.

Alternative splicing of *yki* is required for developmental stability

Despite being viable and fertile, we noticed that several $yki^{2\text{-}only}$ flies in the population display asymmetric wings (Fig 6A). We measured fly wings areas of wild-type and $yki^{2\text{-}only}$ flies, in duplicate to take into account the variability introduced by the manual quantification. This measurement error is low compared with the size difference between right and left wings (Appendix Fig S1). We plotted the distribution of right and left wing sizes of 40 females (Fig 6C, top line) and 40 males (Fig EV5B) in wild type and in the two $yki^{2\text{-}only}$ lines. We noticed an overall reduction of wing size in $yki^{2\text{-}only}$ flies compared with wild type, and an increased difference between right and left sides in several individuals. To quantify the asymmetry between left and right wings, we calculated the fluctuating asymmetry (FA) index FA10 (Palmer & Strobeck, 1986) which takes into account measurement errors. We observed that $yki^{2\text{-}only}$ flies ($yki^{2\text{-}only\text{-}A}$, $yki^{2\text{-}only\text{-}B}$ as well as $yki^{2\text{-}only\text{-}A}/yki^{2\text{-}only\text{-}B}$) display higher FA in both males and females than wild-type controls (Figs 6B and EV5A). The intra-individual variation between the size of right and left wings is recognized as a readout of developmental instability (Palmer, 1994). These results indicate that *yki* alternative splicing is necessary for proper growth equilibration between sides during development.

Increased FA could be the consequence of the loss of Yki1 isoform, could be due to a slight excess of Yki2, or to the loss of alternative splicing regulation. To address this question, we analyzed FA of flies heterozygous for $yki^{2\text{-}only\text{-}A}$ and for a null allele (yki^{B5}) or a wild-type allele (yki^{+}). We observed that $yki^{2\text{-}only\text{-}A}/yki^{B5}$ display FA at a similar level to $yki^{2\text{-}only\text{-}A}$ flies (Fig 6B and C). Since the level of Yki2 is reduced in this context (Fig EV5C), an excess of Yki2 is unlikely responsible for enhanced FA. Combination of $yki^{2\text{-}only\text{-}A}$ with a wild-type allele ($yki^{2\text{-}only\text{-}A}/+$) reduces FA to wild-type levels (Fig 6B and C) suggesting that expression Yki1 isoform is necessary to maintain developmental stability. To further test whether ectopic Yki1 can rescue FA of $yki^{2\text{-}only\text{-}A}$ flies, we overexpressed Yki1 isoform ubiquitously under the control of the *da-Gal4* driver, in homozygous $yki^{2\text{-}only\text{-}A}$ flies. Despite being strongly overexpressed in this context (Fig EV5D), Yki1 protein does not significantly rescue FA of $yki^{2\text{-}only\text{-}A}$ flies (Fig 6B and C), indicating that the mere presence of Yki1 isoform is not sufficient to rescue FA of $yki^{2\text{-}only\text{-}A}$ flies. Finally, to further address the role of AS in these processes, we tested the requirement of B52 by analyzing FA of flies depleted for B52. Ubiquitous expression of B52 RNAi under the control of *da-GAL4* decreases overall wing size and increases FA

Figure 5. Absence of *yki* alternative splicing reduces the phenotype of B52 depletion in the wing and favors clonal growth.

A Structure of the $yki^{2\text{-}only}$ allele compared with wild-type *yki* locus. Introns surrounding exon 3 are removed. This allele does not contain any exogenous sequence.

B Western blot of adult males and females showing disappearance of Yki1 isoform in the two $yki^{2\text{-}only}$ fly lines.

C Comparison of posterior/total area ratio of females wings upon depletion of B52 in a yki^{+} (wild type) or $yki^{2\text{-}only}$ background. Each point corresponds to a single wing, bars represent mean with SD (unpaired two-tailed t-tests: ****P-value < 0.0001).

D Analysis of embryonic lethality according to maternal and paternal genotypes. Bars represent mean and error bars represent SD. Numbers of counted embryos are indicated in each column. Unpaired two-tailed t-tests: ****P-value < 0.0001.

E, F Quantification of sibling clones size in the wing pouch. In (D), sibling wild-type clones are labeled with 2xGFP and 2xRFP. In (E), unlabeled clones are homozygous for the $yki^{2\text{-}only\text{-}A}$ allele whereas sibling clones (RFP/RFP) are wild type. In both graphs, clones pairs are sorted according to RFP/RFP clones size.

Source data are available online for this figure.

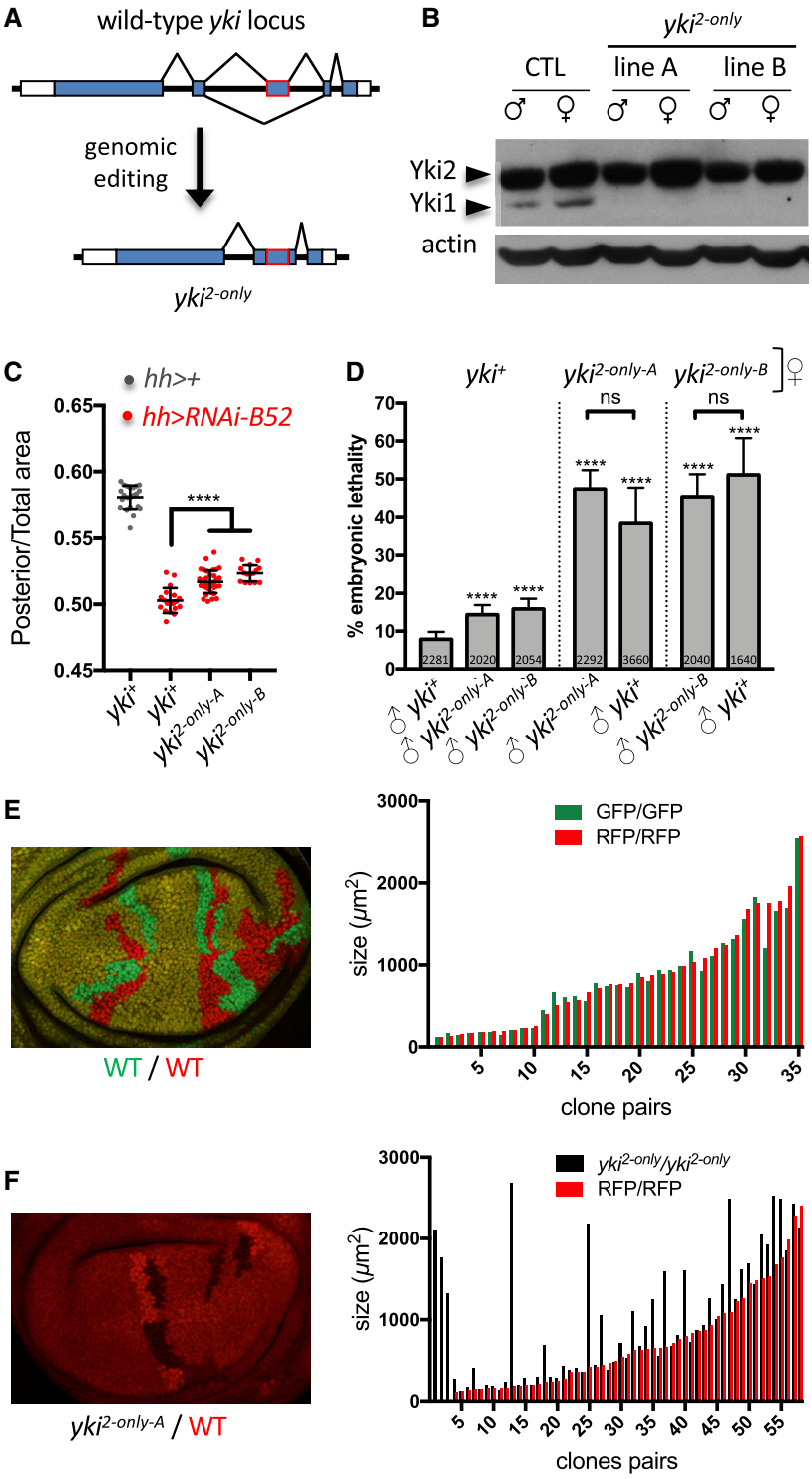

Figure 5.

compared with control flies (*da-GAL4/+*; Fig 6B and C). Unfortunately, we could not test the contribution of *yki* alternative splicing in this context since expression of B52 RNAi in $yki^{2\text{-}only\text{-}A}$ background leads to pupal lethality. Altogether our results strongly suggest that a correct and probably dynamic balance between Yki isoforms, provided by alternative splicing, is necessary for normal equilibration between left and right sides during *Drosophila* development. This is, to our knowledge, the first experimental evidence that alternative splicing participates in the maintenance of developmental stability.

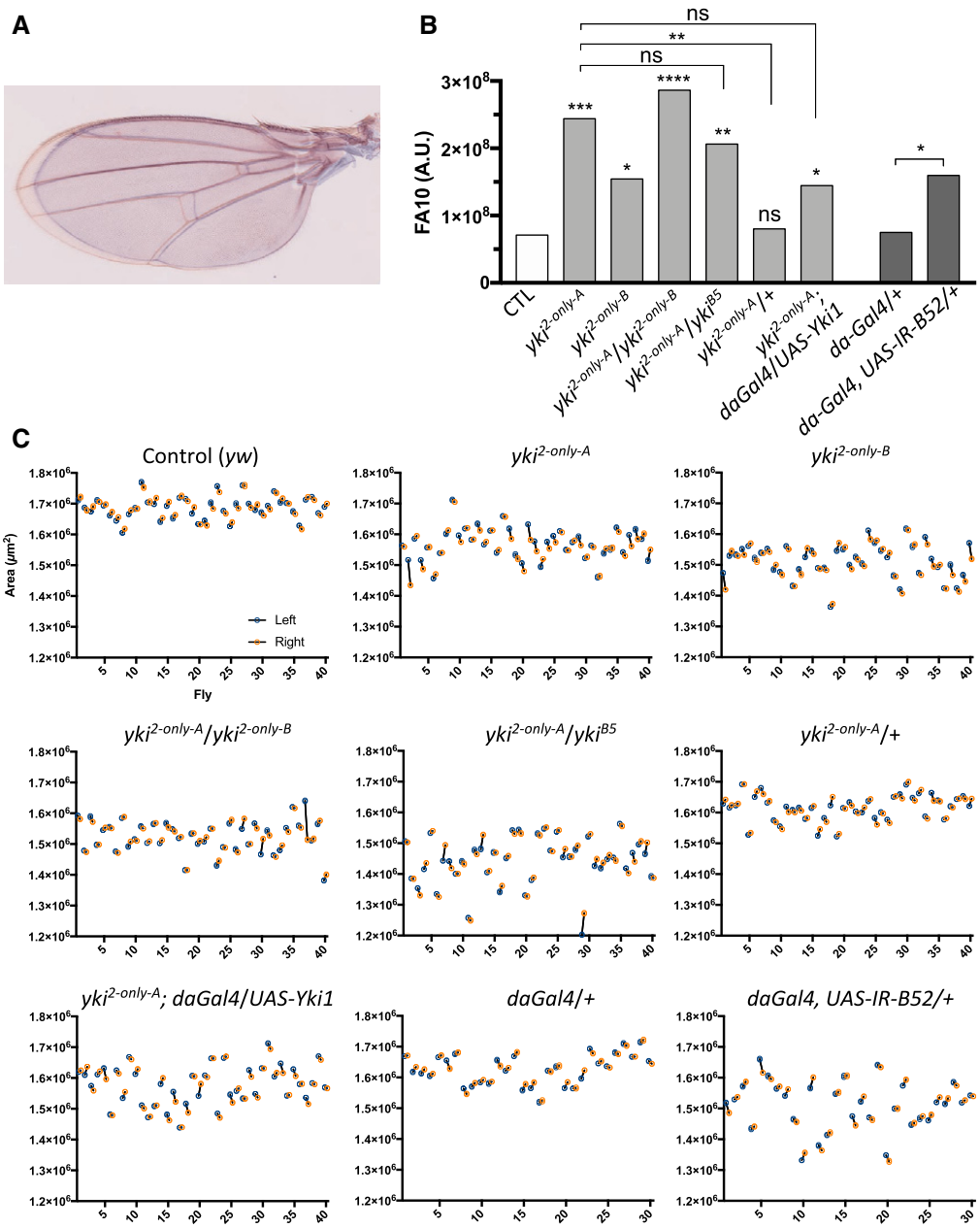

Figure 6. Absence of *yki* alternative splicing increases developmental instability.

A Overlay of right and left wings of a $yki^{2\text{-only-A}}$ female showing fluctuating asymmetry.

B Quantification of fluctuating asymmetry index FA10 in female flies of the indicated genotypes (*F*-tests: **P*-value < 0.05; ***P*-value < 0.01; ****P*-value < 0.001; *****P*-value < 0.0001).

C Distribution of wing size and wing asymmetry among the flies analyzed in panel (B). Each circle represents the area of a single wing. Each wing was measured in duplicate. The difference between right (orange) and left (blue) sides of a single fly is schematized by a black line.

Discussion

Here, we show that alternative splicing of *yki* exon 3 represents an additional layer of modulation of Yki activity that unexpectedly participates in buffering developmental noise. Our results also reveal an important role of Yki1 and/or *yki* alternative splicing for female fertility. We identify the SR protein B52 as the first modulator of *yki* alternative splicing. Significantly, depletion of B52 in the wing reduces growth, and this phenotype is moderately rescued in $yki^{2\text{-only}}$ flies, indicating that B52's effect on growth is in part mediated by its influence on *yki* alternative splicing. B52 depletion induces skipping of *yki* exon 3 and favors the expression of the Yki1 isoform which is a weaker transcriptional activator, compared with the canonical Yki2 isoform. We demonstrate that Yki isoforms

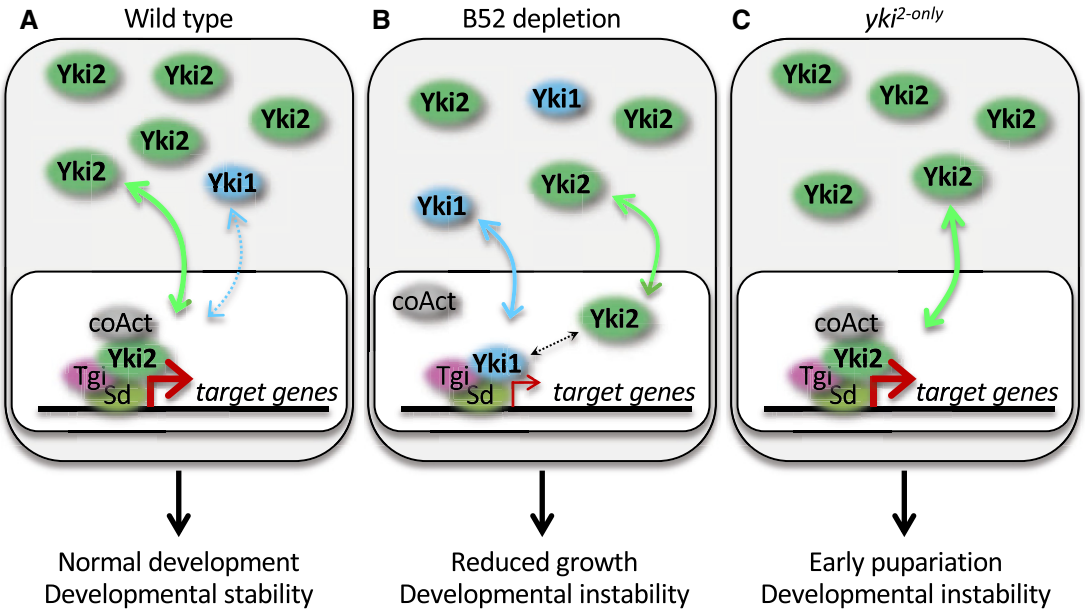

Figure 7. Model: balanced expression of Yki isoforms is necessary for developmental stability.

A In wild-type situation, *yki* alternative splicing allows production of a major fully active isoform Yki2, and a minor isoform Yki1 with reduced activity. This equilibrium contributes to developmental stability.

B B52 depletion reduces *yki* exon3 inclusion level and therefore lowers Yki2/Yki1 ratio. The increased amount of Yki1 enhances its competition with Yki2 for binding to Sd, leading to a decrease of Yki target genes transcription. B52 depletion leads to reduced growth and increased developmental instability.

C In $yki^{2\text{-}only}$ flies, the absence of *yki* alternative splicing causes unbalanced expression of Yki2 isoform which leads to premature pupariation and to increased developmental instability.

interact similarly with transcription factors but differ by their capacity to bind and bridge PPxY-containing proteins. Indeed, Yki1 isoform, which lacks the second WW domain, has reduced interactions with PPxY-containing proteins and lacks the ability to bridge two proteins containing PPxY motifs. These observations allow us to propose the following model (Fig 7). Upon repression of the Hippo pathway, unphosphorylated Yki isoforms accumulate in the nucleus. In a wild-type situation (Fig 7A), the more abundant isoform Yki2 joins the transcriptionally repressed Tgi-Sd complex. Within this trimeric complex, Yki2 may engage only one WW domain with Tgi, thus being able to recruit through the second WW domain another partner such as Wbp2 or NcoA6, which finally may, or not, displace Tgi. This could reconcile the observation that Tgi enhances Sd-Yki interaction but increases the distance between Sd and Yki as measured by FRET (Guo *et al*, 2013) suggesting remodeling of the complex. In a context where B52 is depleted (Fig 7B), Yki2/Yki1 ratio is decreased as a consequence of alternative splicing modulation. Increased level of Yki1 isoform favors its competition with Yki2 for binding to Sd. In a complex with Sd and Tgi, Yki1 would be unable to recruit additional partners and activate transcription, unless Tgi leaves the complex and free the single WW domain. Our results argue that a proper balance between Yki1 and Yki2 isoform is necessary for normal development, since abrogation of *yki* alternative splicing increases developmental instability (Fig 7C). A recent study shows that Yki permanently shuttles between nucleus and cytoplasm (Manning *et al*, 2018), but the two isoforms could not be distinguished in this assay. It would be interesting to compare shuttling properties of Yki isoforms to determine whether different import/export rates could participate in the competition between them.

Somehow surprisingly, despite the fact that $yki^{2\text{-}only}$ cells show growth advantage in clonal assays, $yki^{2\text{-}only}$ flies do not show overgrowth of the wings. We noticed that $yki^{2\text{-}only}$ larvae pupariate slightly before wild-type controls (Appendix Fig S2), suggesting that $yki^{2\text{-}only}$ flies have a slightly accelerated development and probably reduced larval growth phase. It has been shown that, in addition to its intrinsic effect on tissue growth, Yki is involved in systemic growth by interacting with ecdysone signaling. Yki is involved in basal expression of ecdysone (Moeller *et al*, 2017) and interacts with the ecdysone receptor coactivator Taiman (Zhang *et al*, 2015). Alteration of ecdysone signaling in $yki^{2\text{-}only}$ flies may contribute to the earlier pupariation timing and the observed growth defects. In addition, it has been shown that Yki controls the expression of the Dilp8 hormone which is involved in inter-organ coordination of growth (Boone *et al*, 2016). Strong *Dilp8* mutants were shown to display high FA (Garelli *et al*, 2012). Significantly, genomic deletion of *dilp8* Hippo Responsive Element is sufficient to increases FA in flies (Boone *et al*, 2016) indicating that Yki's control on *dilp8* is required to minimize developmental variability. It is possible that abrogation of *yki* alternative splicing alters Yki activity and its control on *dilp8* expression, thus triggering instability. It is likely that the effects observed in $yki^{2\text{-}only}$ animals are a combination of local and global perturbations of growth signals. It will be important to determine to which extent *yki* alternative splicing is dynamically regulated during normal growth and regeneration, and which signals control this regulation.

The splicing factor B52 is a prime candidate to be involved in this process.

Alternative splicing of pre-messenger RNAs is recognized as a major source of transcriptomic and proteomic diversity (Floor & Doudna, 2016; Liu *et al*, 2017). Its extent correlates with organism complexity (Chen *et al*, 2014), and several examples illustrate that alternative splicing is a source of phenotypic novelty during evolution (Bush *et al*, 2017). Here, we provide an experimental evidence that alternative splicing also participates in developmental robustness. Indeed, abrogating a single alternative splicing event in the genome, in the *yki* gene, is sufficient to increase developmental instability in *Drosophila*. Moreover, we observed that ubiquitous depletion of the splicing factor B52 increases FA in the wings. This effect may be linked to alternative splicing changes in *yki* transcripts as well as in other mRNA targets. Interestingly, we identified *Cyclin G* as an alternative splicing target of B52 (Appendix Table S1). The level of Cyclin G protein was previously shown to influence developmental stability (Debat *et al*, 2011). Analyzing the functional consequences of this alternative splicing may reveal another event involved in the maintenance of developmental stability.

It has been proposed that alternative splicing networks created by some splicing regulators participate in the maintenance of transcriptome stability (Jangi & Sharp, 2014). In this view, it is worth noting that B52 tends to control alternative splicing events in genes encoding protein partners (Fig 1B). A similar observation was made for the neuronal-specific splicing factor Nova, which modulates alternative splicing of genes encoding proteins that interact with one another (Ule *et al*, 2005). Such co-regulation could be an efficient strategy to control the activity of specific protein complexes and to maintain cell homeostasis. It is therefore tempting to speculate that master regulators of alternative splicing networks also participate to developmental stability.

Finally, our results highlight *yki* alternative splicing as a new level of modulation of Yki activity. It is worth noting that the alternative inclusion of the second WW domain is a conserved feature between *Drosophila* Yki and human YAP, whereas some characteristics of these proteins, such as the presence of a coiled-coiled domain and a PDZ domain in YAP, are not conserved between the two species. The second WW domain of Yki/YAP appears to reside in a separate exon since the emergence of bilaterians (Hilman & Gat, 2011), suggesting that alternative splicing of this exon could be an ancestral mode of modulation of Yki/YAP activity. Analogously to our results in flies, human YAP isoform containing a single WW domain (YAP1) is a weaker transcriptional activator than the YAP2 isoform containing two WW domains (Komuro *et al*, 2003). Therefore, targeting this alternative splicing event to favor skipping of the alternative exon could be a novel strategy to lower YAP activity that is frequently upregulated in cancer cells (Zanconato *et al*, 2016).

Materials and Methods

RNA-seq analysis

We used MAJIQ (Modeling Alternative Junction Inclusion Quantification) software (v1.0.7) to identify Local Splicing Variations (LSV) in two previously published datasets from Bradley *et al* (2015) (#GSM1552264, #GSM1552267) and Brooks *et al* (2015) (#GSM627333, #GSM627334, and #GSM627343). Each dataset contains two replicates of control and B52-depleted cells RNA-seq. The reads were subjected to standard quality control (QC) and filtered according to the following parameters: (i) trimming and cleaning reads that aligned to primers and/or adaptors, (ii) reads with over 50% of low-quality bases (quality value ≤ 15) in one read, and (iii) reads with over 10% unknown bases (N bases). We used Trimmomatic software (v0.36) to remove primers and bad quality reads. After filtering, we removed short reads (<36bp); the remaining reads are called "clean reads" and stored as FASTQ format. Reads were aligned to *Drosophila melanogaster* reference genome release 6.19 using STAR (Spliced Transcripts Alignment to a Reference) software (v2.5.4b). STAR outputs were stored in BAM files. BAM files were then submitted to MAJIQ analysis pipeline. LSV definitions were generated and quantified by MAJIQ. MAJIQ applies several normalization factors to the raw values before to compute normalized PSI (Percent Selected Index) and compare them between replicates. To make a selection of best candidate genes, we used a ΔPSI threshold of 0.2. All other parameters were used with default values. Gene and PSI lists for each dataset were compared to identify common events between them. This identified 108 alternative splicing events in 105 genes that show reproducible change of alternative splicing upon B52 depletion. GO term analysis was performed with PANTHER (http://pantherdb.org/). Sashimi plots were created with IGV (Integrative Genomics Viewer, https://igv.org/). Protein–protein interactions within the 105 identified genes were tested using Molecular Interaction Search Tool (MIST; http://fgr tools.hms.harvard.edu/MIST/) using the high-confidence threshold which retains only the interactions (direct or indirect) supported by several experimental methods (Hu *et al*, 2018). The number of complexes identified was compared with the distribution of the number of complexes found in 50 sets of 105 random genes, which fits a Poisson distribution ($\lambda = 2.36$).

Fly strains and genetics

Drosophila were maintained on standard cornmeal-yeast medium. Experiments were performed at 25°C, except for the analysis of wing phenotype of flies expressing B52 RNAi under the control of *hh-Gal4* that were performed at 18°C, as mentioned in figure legends. Inducible RNAi lines used were *UAS-IR-B52* (GD8690), *UAS-IR-Wts* (GD1563 and TRiP.HMS00026), *UAS-IR-Hpo* (TRiP.HMS00006), and *UAS-IR-Tgi* (TRiP.HMS00981) and were previously validated in the literature.

UAS-Yki1 and *UAS-Yki1*^{S168A} transgenes were constructed from *pUAS-Yki-V5-His* and *pUAS-Yki*^{S168A}*-V5-His* clones in *pUAS-attB* vector, kindly provided by K. Irvine (these clones contain Yki2 isoform cDNA). A *Xho*I site located between *UAS* sequences and start codon, flanked by two *Eco*RI sites, was deleted by *Eco*RI digestion and re-ligation of these vectors. This generated *UAS-Yki2-V5-His* and *UAS-Yki2*^{S168A}*-V5-His*. The *Sfi*I–*Xho*I fragment containing the C-terminal part of Yki2 was replaced by the corresponding *Sfi*I–*Xho*I amplified from a *yki1* cDNA obtained by RT–PCR (third instar larvae). This generated *UAS-Yki1-V5-His* and *UAS-Yki1*^{S168A}*-V5-His* transgenes. The four constructs *UAS-Yki2-V5-His*, *UAS-Yki2*^{S168A}*-V5-His*, *UAS-Yki1-V5-His,* and *UAS-Yki1*^{S168A}*-V5-His* were inserted in *attP2* landing site through PhiC31-mediated integration. Injections

were performed by Bestgene Inc. In the text, *UAS-Yki* lines are named without the V5-His tag for simplicity.

For immunostainings, the following antibodies were used: mouse anti-ßGal (DSHB), mouse anti-V5 (Invitrogen), and rabbit anti-B52 (Fic *et al*, 2007), using standard procedures. Images were acquired on a Leica SP5 confocal. To compare expression in anterior versus posterior part of wing discs, fluorescence intensity was quantified using OMERO (www.openmicroscopy.org) in an equivalent area in the anterior and posterior domains of the wing pouch, excluding dorsoventral and anterioposterior boundaries. For clonal analyses, larvae were heat shocked during 30 min at 37°C, either 48 h ± 4 or 72 h ± 4 after egg laying, and then dissected 48, 68, or 72 h after clone induction. Areas of clones were quantified in the wing pouch with OMERO.

For quantification of pupariation timing, first instar larvae of the appropriate genotypes were collected 24–28 h after egg laying and reared at 30 larvae per tube at 25°C. Two independent experiments were performed, and in total, 17 tubes were counted for each genotype.

The detail of genotypes used in each Figure is given in Appendix Table S2.

yorkie gene editing

To edit endogenous *yki* locus by CRISPR/Cas9-mediated homologous recombination, a repair construct corresponding to *yki* gene without introns 2 and 3, and containing a piggyBac insertion in intron 1, was created by cloning of multiple PCR fragments amplified with Q5-Taq polymerase (NEB). *yki* gene fragments were amplified from *yw* flies. The piggyBac transposon containing the reporter gene *3xP3-DsRed* (expresses DsRed in the eye) was amplified from *pHD-3xFLAG-ScarlessDsRed* (http://flycrispr.molbio.wisc.edu/scarless; DGRC #1367) and cloned into a *Dra*I site present in *yki* intron 1, thus creating TTAA sequences at both sides of the transposon that are necessary for its excision. We used two guide RNAs targeting exon 2 and exon 4 of *yki*, cloned into pCFD4 (addgene #49411). The plasmid containing the repair construct was co-injected with the plasmid encoding the two guides into *nos-Cas9* embryos. Injection and screening for positive DsRED flies in the progeny were performed by Bestgene Inc. Two DsRED-positive lines, validated by PCR, were selected for excision of piggyBac transposon using a source of transposase (Bloomington #8285). For each line, a single excision event was selected to establish a stock. Two independent $yki^{2\text{-}only}$ alleles were obtained, called *A* and *B*. The entire *yki* locus was sequenced in these lines. We detected polymorphism in introns and silent polymorphism in exons. These differences are present between the *yw* line used to create the $yki^{2\text{-}only}$ construct and the *nos-Cas9* line in which the injections were made. Both $yki^{2\text{-}only}$ lines gave similar results.

Molecular biology

cDNAs corresponding to MAD, GAF, Sd, Hth, 14.3.3, Hpo, and Wbp2 were amplified from third instar larvae RNA by RT–PCR, using a forward primer starting at ATG and reverse primer located just upstream (or sometimes including) the stop codon. Forward primer contains CACC sequence upstream from ATG to orient cloning in pENTR/D-Topo (Invitrogen). All cDNAs were entirely sequenced. Other cDNAs were Cabut (DmCD00765693, DNASU), Tgi (DmCD00765105, DNASU), Mor (Addgene #71048), and Ex (kindly provided by N. Tapon). NcoA6 was amplified from a plasmid kindly provided by K. Irvine. Yki isoforms fused to Gal4 DNA binding domain (G4DBD) were kindly provided by N. Tapon.

For DUAL-luciferase co-IP, we developed three destination vectors for the Gateway system: pAct-Flag-Firefly-RfA, pAct-HA-Renilla-RfA, and pAct-RfB-Renilla-HA. The luciferase-gateway cassettes from mammalian vectors pcDNA-Flag-Firefly-RfA, pcDNA5-HA-Renilla-RfA, and pcDNA5-RfB-Renilla-HA (kindly provided by E. Bertrand) were cloned between *Kpn*I and *Nhe*I sites of *pAFW* vector backbone (Drosophila Genomics Resource Center). cDNAs cloned into pENTR/D-Topo were transferred to the appropriate destination vector by LR recombination (Invitrogen). Mutations of the two WW domains were introduced in Yki2 cDNA cloned in pENTR/D-Topo with Q5 Site-Directed Mutagenesis Kit (Biolabs). The sequence WxxP in each WW domain was mutated into FxxA to abolish binding without strongly modifying its structure (Chen *et al*, 1997).

Cell culture and co-immunoprecipitations

Drosophila S2R+ cells were maintained in Schneider's medium (Invitrogen) supplemented with 10% fetal bovine serum (Sigma), 50 U/ml penicillin, and 50 µg/ml streptomycin (Invitrogen) at 27°C. For B52 depletion, S2R+ cells were treated with a mix of two dsRNA (produced by *in vitro* transcription) targeting exon 2 and exon 9 of *B52*, for 72H. RNAs were extracted with TRIzol (Sigma). Proteins were prepared in urea buffer (63 mM Tris–HCl pH7.5, 2% SDS, 5% 2-mercaptoethanol, 8M urea). Primary antibodies used for western were rabbit anti-Yki (Oh & Irvine, 2008), rat anti-B52 (Juge *et al*, 2010), and mouse anti-actin (DSHB).

For luciferase assays, S2R+ cells were transfected for 48 h (or 24 h for competition assay, Fig 4G) in triplicates using effectene, in 96-well plate. *Copia-Renilla* was used as normalizer, and luciferase activities were quantified with DUAL luciferase reporter assay (Promega).

For dual-luciferase co-IP, S2R+ cells were transfected with two plasmids (0.15 µg each), in quadruplicate, in 24-wells plates (400,000 cells/well) using effectene (Qiagen). Typically, four plates were handled at the same time to perform 24 co-IPs in quadruplicate. After 48 h of transfection, cells were washed with PBS and lysed with 250 µl HNTG buffer (20 mM Hepes pH 7.9, 150 mM NaCl, 1 mM $MgCl_2$, 1 mM EDTA, 1% Triton, 10% glycerol) supplemented with proteases inhibitors (Halt inhibitor cocktail, Thermo Scientific). Immunoprecipitation (IP) were performed on each lysate in 96-wells Neutravidin plates (Thermo Scientific) previously coated for 2 h with biotinylated anti-Flag antibody (Bio-M2, Sigma) in HNTG (2 µg antibody/well). IP were performed with 100 µl of lysate/well and incubated overnight at 4°. IP were washed five times with 200 µl HNTG/well for 5 min at 20° on a thermomixer (Eppendorf) with intermittent shacking. Firefly luciferase (FL) and Renilla luciferase (RL) activities were then quantified with DUAL luciferase reporter assay (Promega) using 50 µl of reagents/well and an InfiniteF200 reader (TECAN). To quantify input, 10 µl of each lysate were transferred in a white 96-well plate and quantified as the same time as IP plate with the same procedure. The level of co-IP is quantified by calculating the level of co-IP normalized to the

efficiency of IP: coIP = $(RL^{IP}/RL^{Input})/(FL^{IP}/FL^{Input})$. For each prey tested, a control co-IP using Flag-Firefly (FFL) as bait was performed and used as reference (interaction set to 1). Each coIP value was normalized to the mean of the quadruplicate control co-IP: NcoIP = $coIP^{FFL\text{-}bait}/MEAN(coIP^{FFL})$.

For bridging experiments between a FL-tagged bait and a RL-tagged prey, in absence or presence of Yki isoforms, the same procedure was used with a co-transfection of 0.15 μg of Firefly plasmid, 0.15 μg Renilla plasmid, and 0.3 μg pAct-Myc-Yki plasmid (or a control plasmid expressing GFP for control without Yki). Transfections and IPs were performed in quadruplicate as described above. Interaction detected in the absence of Yki was used as reference to calculate the normalized co-IP ratio NcoIP. In all co-IP, results represent mean ± s.e.m. Student's *t*-tests (unpaired two-tailed) were performed using GraphPad Prism and illustrated as: **P*-value < 0.05, ***P*-value < 0.01, ****P*-value < 0.001, *****P*-value < 0.0001.

Wing measurements

For measurements of posterior versus total area (experiments with *hh-Gal4* driver), young flies (1–3 days) of the appropriate genotypes were stored in isopropanol. Wings were mounted in Euparal (Carl Roth GmbH) on glass slide with coverslip and baked overnight at 65°. Pictures were acquired on a Leica M80 stereomicroscope equipped with a Leica IC80 HD camera using LAS software. Measurements were performed with OMERO (www.openmicroscopy.org).

For quantification of Fluctuating Asymmetry (FA), adult flies were collected at 25° from tubes with controlled population density (either 30 larvae per tube or short egg-laying period), stored in isopropanol and their left and right wings were mounted as pairs in Euparal. Slides were digitalized using Nanozoomer (Hamamatsu). Measurements of wing areas were performed with ImageJ. Each wing was measured twice in two independent sessions, by one or two persons. In rare cases where the variation between replicate measurements was superior to 0.5% of total wing area, the wing was quantified again to minimize measurement error. The FA10 index was used to estimate FA, i.e., FA corrected for measurement error, directional asymmetry, and inter-individual variation (Palmer & Strobeck, 1986). For all genotypes, the interaction individual/side was significant, indicating that FA was larger than measurement error (Fig S5). Conventional two-way mixed-model ANOVAs were applied to areas data using GraphPad Prism Software. These values were used to calculate FA10 index: $FA10=(MS_{Interaction}-MS_{Residual})/2$. To compare FA10 values between genotypes, we used *F*-test to compare variance of the samples.

Data availability

This study includes no data deposited in external repositories.

Expanded View for this article is available online.

Acknowledgements
We thank Nicolas Tapon for helpful comments on the manuscript and Thierry Gostan for his advice on statistical analyses. We thank Kenneth Irvine, Nicolas Tapon, Alexandre Djiane, and Edouard Bertrand for sharing flies, constructs, and antibodies. We thank the Montpellier RIO Imaging facility for microscopy. We acknowledge the Bloomington Drosophila Stock Center for providing flies stocks, the Developmental Studies Hybridoma Bank (DSHB) for antibodies, and the Drosophila Genomics Resource Center (DGRC), DNASU and Addgene for plasmids. DS was supported by a PhD fellowship from la Ligue Nationale Contre le Cancer.

Author contributions
Genetic experiments and wing quantifications: DS and FJ; Immunostainings and associated quantifications: DS; Experiments with S2 cells: MT and FJ; RNA-seq and splicing analyses: LM; Project finance: JT; Project design and manuscript writing: FJ.

Conflict of interest
The authors declare that they have no conflict of interest.

References

Badouel C, Gardano L, Amin N, Garg A, Rosenfeld R, Le Bihan T, McNeill H (2009) The FERM-domain protein Expanded regulates Hippo pathway activity via direct interactions with the transcriptional activator Yorkie. *Dev Cell* 16: 411 – 420

Boone E, Colombani J, Andersen DS, Léopold P (2016) The Hippo signalling pathway coordinates organ growth and limits developmental variability by controlling dilp8 expression. *Nat Commun* 7: 13505

Bradley T, Cook ME, Blanchette M (2015) SR proteins control a complex network of RNA-processing events. *RNA* 21: 75 – 92

Brooks AN, Duff MO, May G, Yang L, Bolisetty M, Landolin J, Wan K, Sandler J, Booth BW, Celniker SE *et al* (2015) Regulation of alternative splicing in Drosophila by 56 RNA binding proteins. *Genome Res* 25: 1771 – 1780

Bush SJ, Chen L, Tovar-Corona JM, Urrutia AO (2017) Alternative splicing and the evolution of phenotypic novelty. *Philos Trans R Soc B Biol Sci* 372: 20150474

Chen HI, Einbond A, Kwak SJ, Linn H, Koepf E, Peterson S, Kelly JW, Sudol M (1997) Characterization of the WW domain of human yes-associated protein and its polyproline-containing ligands. *J Biol Chem* 272: 17070 – 17077

Chen L, Bush SJ, Tovar-Corona JM, Castillo-Morales A, Urrutia AO (2014) Correcting for differential transcript coverage reveals a strong relationship between alternative splicing and organism complexity. *Mol Biol Evol* 31: 1402 – 1413

Debat V, Bloyer S, Faradji F, Gidaszewski N, Navarro N, Orozco-Terwengel P, Ribeiro V, Schlötterer C, Deutsch JS, Peronnet F (2011) Developmental stability: a major role for cyclin G in drosophila melanogaster. *PLoS Genet* 7: e1002314

Dong J, Feldmann G, Huang J, Wu S, Zhang N, Comerford SA, Gayyed MF, Anders RA, Maitra A, Pan D (2007) Elucidation of a universal size-control mechanism in Drosophila and mammals. *Cell* 130: 1120 – 1133

Elosegui-Artola A, Andreu I, Beedle AEM, Lezamiz A, Uroz M, Kosmalska AJ, Oria R, Kechagia JZ, Rico-Lastres P, Le Roux A-L *et al* (2017) Force triggers YAP nuclear entry by regulating transport across nuclear pores. *Cell* 171: 1397 – 1410

Fernando C, Audibert A, Simon F, Tazi J, Juge F (2015) A Role for the serine/arginine-rich (SR) protein B52/SRSF6 in cell growth and Myc expression in *Drosophila*. *Genetics* 199: 1201 – 1211

Fic W, Juge F, Soret J, Tazi J (2007) Eye development under the control of SRp55/B52-mediated alternative splicing of eyeless. *PLoS One* 2: e253

Floor SN, Doudna JA (2016) Tunable protein synthesis by transcript isoforms in human cells. *eLife* 5: 1276

Garelli A, Gontijo AM, Miguela V, Caparros E, Dominguez M (2012) Imaginal discs secrete insulin-like peptide 8 to mediate plasticity of growth and maturation. *Science* 336: 579 – 582

Goulev Y, Fauny JD, Gonzalez-Marti B, Flagiello D, Silber J, Zider A (2008) SCALLOPED interacts with YORKIE, the nuclear effector of the hippo tumor-suppressor pathway in *Drosophila*. *Curr Biol* 18: 435 – 441

Guo T, Lu Y, Li P, Yin M-X, Lv D, Zhang W, Wang H, Zhou Z, Ji H, Zhao Y *et al* (2013) A novel partner of Scalloped regulates Hippo signaling via antagonizing Scalloped-Yorkie activity. *Cell Res* 23: 1201 – 1214

Harvey KF, Pfleger CM, Hariharan IK (2003) The Drosophila Mst ortholog, hippo, restricts growth and cell proliferation and promotes apoptosis. *Cell* 114: 457 – 467

Hilman D, Gat U (2011) The evolutionary history of YAP and the hippo/YAP pathway. *Mol Biol Evol* 28: 2403 – 2417

Howard JM, Sanford JR (2015) The RNAissance family: SR proteins as multifaceted regulators of gene expression. *Wiley Interdiscip Rev RNA* 6: 93 – 110

Hu Y, Vinayagam A, Nand A, Comjean A, Chung V, Hao T, Mohr SE, Perrimon N (2018) Molecular Interaction Search Tool (MIST): an integrated resource for mining gene and protein interaction data. *Nucleic Acids Res* 46: D567 – D574

Huang J, Wu S, Barrera J, Matthews K, Pan D (2005) The Hippo signaling pathway coordinately regulates cell proliferation and apoptosis by inactivating Yorkie, the Drosophila Homolog of YAP. *Cell* 122: 421 – 434

Jangi M, Sharp PA (2014) Building robust transcriptomes with master splicing factors. *Cell* 159: 487 – 498

Jia J, Zhang W, Wang B, Trinko R, Jiang J (2003) The Drosophila Ste20 family kinase dMST functions as a tumor suppressor by restricting cell proliferation and promoting apoptosis. *Genes Dev* 17: 2514 – 2519

Juge F, Fernando C, Fic W, Tazi J (2010) The SR protein B52/SRp55 is required for DNA topoisomerase I recruitment to chromatin, mRNA release and transcription shutdown. *PLoS Genet* 6: e1001124

Justice RW, Zilian O, Woods DF, Noll M, Bryant PJ (1995) The Drosophila tumor suppressor gene warts encodes a homolog of human myotonic dystrophy kinase and is required for the control of cell shape and proliferation. *Genes Dev* 9: 534 – 546

Komuro A, Nagai M, Navin NE, Sudol M (2003) WW domain-containing protein YAP associates with ErbB-4 and acts as a co-transcriptional activator for the carboxyl-terminal fragment of ErbB-4 that translocates to the nucleus. *J Biol Chem* 278: 33334 – 33341

Koontz LM, Liu-Chittenden Y, Yin F, Zheng Y, Yu J, Huang B, Chen Q, Wu S, Pan D (2013) The Hippo effector Yorkie controls normal tissue growth by antagonizing scalloped-mediated default repression. *Dev Cell* 25: 388 – 401

Liu Y, Gonzàlez-Porta M, Santos S, Brazma A, Marioni JC, Aebersold R, Venkitaraman AR, Wickramasinghe VO (2017) Impact of alternative splicing on the human proteome. *Cell Rep* 20: 1229 – 1241

Manning SA, Dent LG, Kondo S, Zhao ZW, Plachta N, Harvey KF (2018) Dynamic fluctuations in subcellular localization of the hippo pathway effector Yorkie in vivo. *Curr Biol* 28: 1651 – 1660

Misra JR, Irvine KD (2018) The hippo signaling network and its biological functions. *Annu Rev Genet* 52: 65 – 87

Moeller ME, Nagy S, Gerlach SU, Soegaard KC, Danielsen ET, Texada MJ, Rewitz KF (2017) Warts signaling controls organ and body growth through regulation of ecdysone. *Curr Biol* 27: 1652 – 1659

Nyarko A (2018) Differential binding affinities and allosteric conformational changes underlie interactions of Yorkie and a multivalent PPxY partner. *Biochemistry* 57: 547 – 556

Oh H, Irvine KD (2008) In vivo regulation of Yorkie phosphorylation and localization. *Development* 135: 1081 – 1088

Oh H, Reddy BVVG, Irvine KD (2009) Phosphorylation-independent repression of Yorkie in Fat-Hippo signaling. *Dev Biol* 335: 188 – 197

Oh H, Slattery M, Ma L, White KP, Mann RS, Irvine KD (2014) Yorkie promotes transcription by recruiting a histone methyltransferase complex. *Cell Rep* 8: 449 – 459

Oka T, Mazack V, Sudol M (2008) Mst2 and Lats kinases regulate apoptotic function of Yes kinase-associated protein (YAP). *J Biol Chem* 283: 27534 – 27546

Oka T, Schmitt AP, Sudol M (2012) Opposing roles of angiomotin-like-1 and zona occludens-2 on pro-apoptotic function of YAP. *Oncogene* 31: 128 – 134

Palmer AR, Strobeck C (1986) FLUCTUATING ASYMMETRY: measurement, analysis, patterns. *Ann Rev Ecol Syst* 17: 391 – 421

Palmer AR (1994) Fluctuating asymmetry analyses: a primer. In *Developmental Instability Its Origins and Evolutionary Implications. Contemporary Issues in Genetics and Evolution*, Markov TA (ed), pp 335 – 364. Dordrecht: Springer

Pantalacci S, Tapon N, Léopold P (2003) The Salvador partner Hippo promotes apoptosis and cell-cycle exit in Drosophila. *Nat Cell Biol* 5: 921 – 927

Qing Y, Yin F, Wang W, Zheng Y, Guo P, Schozer F, Deng H, Pan D (2014) The Hippo effector Yorkie activates transcription by interacting with a histone methyltransferase complex through Ncoa6. *eLife* 3: 1260

Trepte P, Buntru A, Klockmeier K, Willmore L, Arumughan A, Secker C, Zenkner M, Brusendorf L, Rau K, Redel A *et al* (2015) DULIP: a dual luminescence-based co-immunoprecipitation assay for interactome mapping in mammalian cells. *J Mol Biol* 427: 3375 – 3388

Udan RS, Kango-Singh M, Nolo R, Tao C, Halder G (2003) Hippo promotes proliferation arrest and apoptosis in the Salvador/Warts pathway. *Nat Cell Biol* 5: 914 – 920

Ule J, Ule A, Spencer J, Williams A, Hu J-S, Cline M, Wang H, Clark T, Fraser C, Ruggiu M *et al* (2005) Nova regulates brain-specific splicing to shape the synapse. *Nat Genet* 37: 844 – 852

Vaquero-Garcia J, Barrera A, Gazzara MR, González-Vallinas J, Lahens NF, Hogenesch JB, Lynch KW, Barash Y (2016) A new view of transcriptome complexity and regulation through the lens of local splicing variations. *eLife* 5: e11752

Webb C, Upadhyay A, Giuntini F, Eggleston I, Furutani Seiki M, Ishima R, Bagby S (2011) Structural features and ligand binding properties of tandem WW domains from YAP and TAZ, nuclear effectors of the Hippo pathway. *Biochemistry* 50: 3300 – 3309

Wu S, Huang J, Dong J, Pan D (2003) hippo encodes a Ste-20 family protein kinase that restricts cell proliferation and promotes apoptosis in conjunction with salvador and warts. *Cell* 114: 445 – 456

Wu S, Liu Y, Zheng Y, Dong J, Pan D (2008) The TEAD/TEF family protein Scalloped mediates transcriptional output of the Hippo growth-regulatory pathway. *Dev Cell* 14: 388 – 398

Xu T, Wang W, Zhang S, Stewart RA, Yu W (1995) Identifying tumor suppressors in genetic mosaics: the Drosophila lats gene encodes a putative protein kinase. *Development* 121: 1053 – 1063

Zanconato F, Cordenonsi M, Piccolo S (2016) YAP/TAZ at the roots of cancer. *Cancer Cell* 29: 783 – 803

Zhang L, Ren F, Zhang Q, Chen Y, Wang B, Jiang J (2008) The TEAD/TEF family of transcription factor Scalloped mediates Hippo signaling in organ size control. *Dev Cell* 14: 377 – 387

Zhang X, Milton CC, Poon CLC, Hong W, Harvey KF (2011) Wbp2 cooperates with Yorkie to drive tissue growth downstream of the Salvador-Warts-Hippo pathway. *Cell Death Differ* 18: 1346 – 1355

Zhang C, Robinson BS, Xu W, Yang L, Yao B, Zhao H, Byun PK, Jin P, Veraksa A, Moberg KH (2015) The ecdysone receptor coactivator Taiman links Yorkie to transcriptional control of germline stem cell factors in somatic tissue. *Dev Cell* 34: 168 – 180

Zhao B, Wei X, Li W, Udan RS, Yang Q, Kim J, Xie J, Ikenoue T, Yu J, Li L *et al* (2007) Inactivation of YAP oncoprotein by the Hippo pathway is involved in cell contact inhibition and tissue growth control. *Genes Dev* 21: 2747 – 2761

Zhao B, Ye X, Yu J, Li L, Li W, Li S, Yu J, Lin JD, Wang C-Y, Chinnaiyan AM *et al* (2008) TEAD mediates YAP-dependent gene induction and growth control. *Genes Dev* 22: 1962 – 1971

Zheng Y, Pan D (2019) The Hippo signaling pathway in development and disease. *Dev Cell* 50: 264 – 282

